Raman Spectroscopic Study of the Concentration Phase Transition in $Pb_{1-x}Ca_xTiO_3$ Solid Solutions

V. I. Torgashev[a], Yu. I. Yuzyuk[a], V. V. Lemanov[b], and C. A. Kuntscher[c]

[a] *Rostov State University, pr. Stachki 194, Rostov-on-Don, 344090 Russia*

e-mail: victor@ip.rsu.ru

[b] *Ioffe Physicotechnical Institute, Russian Academy of Sciences, Politekhnicheskaya ul. 26, St. Petersburg, 194021 Russia*

[c] *Physikalisches Institut, Universität Stuttgart, Pfaffenwaldring 57, Stuttgart, D-70550 Germany*

1. INTRODUCTION

Solid solutions of $Pb_{1-x}Ca_xTiO_3$ (PCT) perovskites experience a complex structural evolution with a variation in the concentration x, because the compounds forming these solid solutions ($CaTiO_3$, $PbTiO_3$) have different symmetry at room temperature.

At high temperatures ($T > 1580$ K), calcium titanate $CaTiO_3$ has cubic space group $Pm\bar{3}m–O_h^1$. As the temperature decreases, $CaTiO_3$ undergoes a sequence of antiferrodistorsive phase transitions (among the conceivable sequences are, for example, $Pm\bar{3}m \longrightarrow I4/mcm \longrightarrow Cmcm$ (or $Imma$) $\longrightarrow Pnma$), the temperatures and intermediate phase symmetries of which have not, however, been thus far reliably established [1–4]. At $T < 1380$ K, structural transformations are stabilized within orthorhombic symmetry $Pnma–D_{2h}^{16}$ with the unit cell parameters $a = 5.444$ Å, $b = 7.644$ Å, $c = 5.367$ Å, and $Z = 4$ (formula units) [4, 5]. All the low-symmetry distortions are caused by the condensation of soft modes from the R and M points of the cubic Brillouin zone with the inclusion of secondary order parameters [6].

During cooling from room temperature to liquid-helium temperature, the static permittivity of $CaTiO_3$ increases hyperbolically from 170 to 330 [7] and, at 40 K, reaches saturation; however, the crystal still does not transform into a polar phase state. From the standpoint of dynamic theory of ferroelectricity, this behavior of the static permittivity implies that $CaTiO_3$ exhibits a lattice instability in the form of a polar soft mode

and a trend to a ferroelectric phase transition. The corresponding behavior of phonon modes in IR reflectance spectra with a variation in temperature was indeed observed in [8, 9].

Lead titanate $PbTiO_3$ undergoes a $Pm\bar{3}m \rightleftarrows P4mm$ phase transition at 763 K [10]. This transition was studied comprehensively as a model that could shed light on the mechanisms of phase transitions of displacive type [11–17]. It is driven by an unstable soft phonon mode of F_{1u} symmetry from the center of the cubic Brillouin zone [11–15]. In the immediate vicinity of the Curie point, however, $PbTiO_3$ exhibits a weak order–disorder-type behavior [16, 17]. Comprehensive studies of Raman scattering spectra of a $PbTiO_3$ single crystal [11] permitted assignment of all Raman-active modes in the tetragonal phase and revealed that the behavior of the lowest frequency transverse phonon $E(1TO)$ is characteristic of a soft mode. Moreover, Burns and Scott [11] showed that the model of a damped oscillator with a frequency-independent damping coefficient describes well the shape of the E mode profile at temperatures up to $T_c = 766$ K. The assignment of the $A_1(1TO)$ phonon was first made by Fontana et al. [17], but without interpretation of its anomalous spectral shape. The shape of the $A_1(1TO)$ component of the F_{1u} soft mode was later studied in considerable detail in [13, 18], and a model assuming a double-minimum potential and adequately describing its spectral profile was proposed. Quite recently, Cho et al. [19] performed a thorough analysis and drew the conclusion that the anomalous scattering intensity at the lowest frequency soft subpeak of the $A_1(1TO)$ mode, rather than
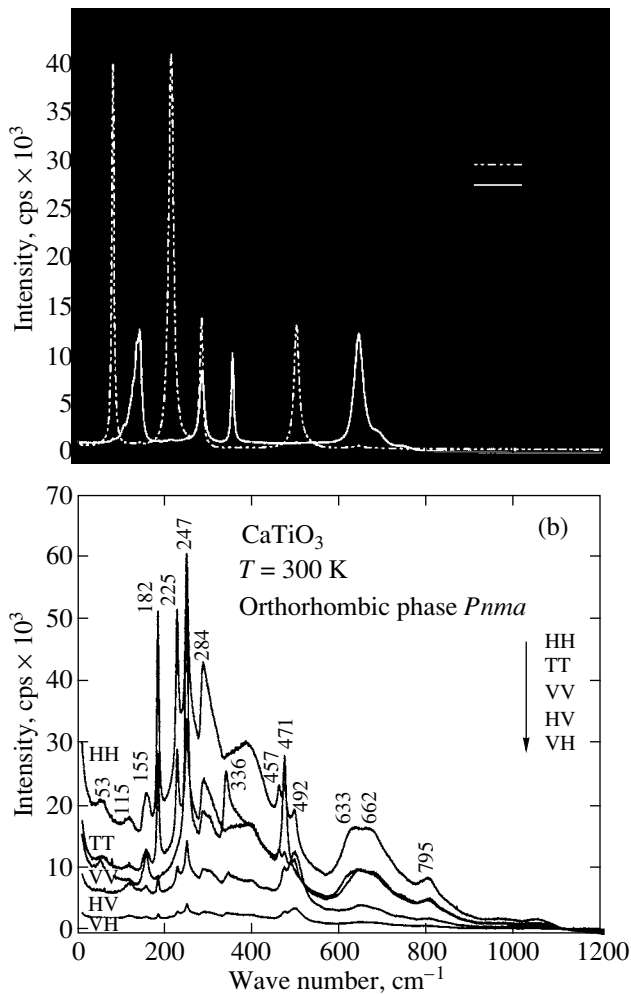
Fig. 1. Polarized Raman spectra of (a) PbTiO₃ and (b) CaTiO₃ single crystals at room temperature. The mode assignment for lead titanate is made as described in [11, 12]. The spectrum of orthorhombic calcium titanate is slightly depolarized because of the complex domain structure of the sample.

being related directly to the anharmonicity of the double-minimum potential, originates actually from thermodynamically stable lattice defects.

The PCT solid solutions exhibit a strong piezoelectric effect and good ferroelectric and pyroelectric properties [20–22] in the bulk and thin-film realizations, which underpins their diverse practical applications [23–26]. Moreover, addition of such elements as strontium, barium, or calcium to lead titanate decreases significantly the Curie temperature, thus permitting a variation in the operating temperature range of electronic devices. This accounts for the interest that the investigation of the variation in their properties with composition arouses from both the purely scientific and practical standpoints. Still, some points remain in this respect unclear. For example, relaxor behavior was revealed at some concentrations x [27]. On the other hand, neutron
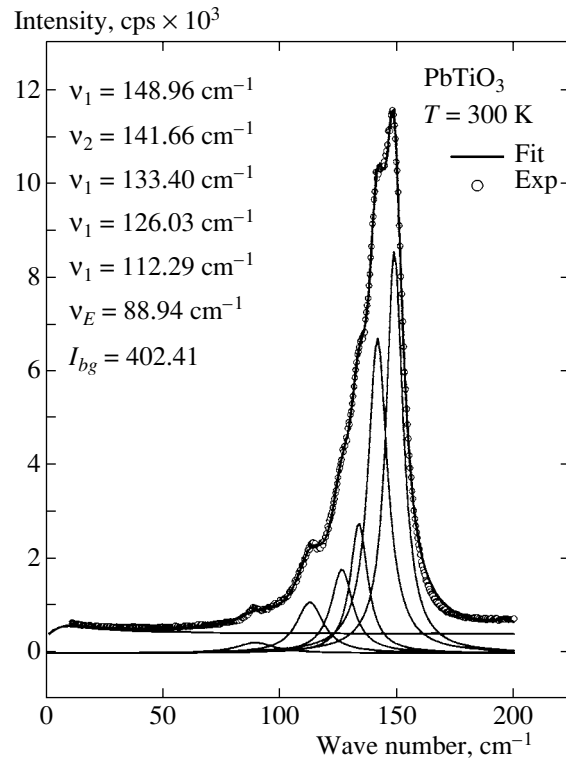
Fig. 2. Spectral profile of the $A_1(1TO)$ soft mode in a PbTiO₃ crystal at room temperature and its deconvolution into additive components, which reveals a strongly anharmonic character of this phonon mode. Numerical values of the eigenfrequencies of the constituent profiles obtained by fitting the spectra with model (1) are presented.

diffraction measurements showed the $(Ca_{0.5}Pb_{0.5})TiO_3$ structure to be orthorhombically distorted through tilting of octahedra and displacements of Pb^{2+}/Ca^{2+} ions from the central perovskite sites, the symmetry of this solid solution being the same as that of the calcium titanate ($Pnma–D_{2h}^{16}$) [28]. According to Ganesh and Goo [29], the structure remains orthorhombic at $x = 0.9$ and 0.8, but the solid solution becomes pseudocubic at $x = 0.7$ and 0.6 (with orthorhombic distortions decreasing substantially) and tetragonal at $x < 0.5$. Eremkin et al. [30] carried out optical investigations of PCT crystals and constructed the $x–T$ diagram for compositions in the concentration range $0 < x < 0.62$ [30]. At medium concentrations, the phase diagram was found to be fairly complex. A complex behavior of PCT solid solutions with a variation in the concentration on the microlevel has been recently established by IR and submillimeter spectroscopy for compositions with high calcium contents [31].

In this paper, we report on the results of analyzing the polarized Raman scattering spectra and dielectric spectra of single-crystal PCT samples ($x = 0$, 0.03, 0.04, 0.15, 0.23, 0.28, 0.34, 0.38, 0.40, 0.45, 0.50) in the frequency range $6 < \nu < 1200$ cm⁻¹ at temperatures of 290–

620 K. The results obtained are compared with data derived from Raman spectra of polycrystalline powders of similar compositions [32].

2. SAMPLE PREPARATION AND EXPERIMENTAL TECHNIQUE

Crystals were grown according to the technique proposed in [30] for crystallizing platelet-shaped PCT solid solutions. The samples thus obtained were transparent crystals of high optical quality in the form of platelets up to 3×4 mm in area and from 10 to 200 μm thick. The composition of the single crystals was determined using a Camebax-Micro scanning electron microscope–microanalyzer with a ZAF quantification. The content of impurities was less than 0.10–0.15 mol %. X-ray diffraction analysis showed that the samples had a single-phase composition. The samples suitable for the studies were naturally grown platelets and were not subjected to any mechanical treatment.

The Raman spectra were excited by polarized radiation from a Coherent-Innova 90 Ar$^+$ ion laser (λ = 514.5 nm) and analyzed on a Jobin Yvon T64000 spectrometer equipped with a CCD camera. The polarized spectra were measured in backscattering geometry with the use of a microscope focusing the light incident on the sample, thus making it possible to collect data on scattering from a spot approximately 2 μm in diameter. A Linkam TS 1500 cell providing a stability of ±1.5 K was employed in high-temperature measurements.

The submillimeter transmittance spectra in the frequency range 3–18 cm^{-1} and IR reflectance spectra in the range 30–10000 cm^{-1} for a PCT45 crystal ($x = 0.45$) at room temperature were recorded on a laboratory Epsilon BWO spectrometer and a Bruker-113V Fourier-transform infrared spectrometer, respectively. For more details of the measurements, the reader can be referred to [31].

Quantitative information on the parameters of phonon modes was gained by invoking the model of additive damped harmonic oscillators. The spectra were least-squares fitted with the relation

$$I(\nu) = I_{ph} + C\left(\frac{1}{e^{h\nu/kT}-1}+1\right)$$
$$\times\left(\frac{\Delta\varepsilon_r\nu\gamma_r}{\nu^2+\gamma_r^2}+\sum_i\frac{\Delta\varepsilon_i\nu_i^2\nu\gamma_i}{(\nu_i^2-\nu^2)^2+\gamma_i^2\nu^2}\right), \quad (1)$$

where I_{ph} is a constant background, C is a constant, ν_i is the eigenfrequency of the ith mode, γ_i is the damping constant of the ith mode, $\Delta\varepsilon_i\nu_i^2$ is the oscillator strength of the ith mode, γ_r is the inverse relaxation time, and $\Delta\varepsilon_r$ is the relaxation contribution to the static permittivity.
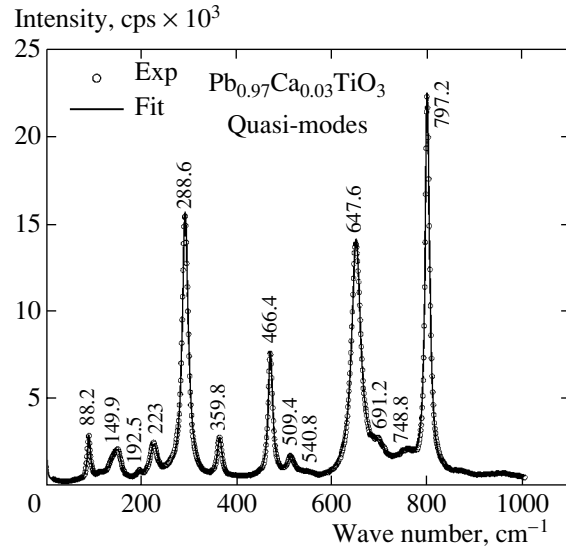
Fig. 3. Illustration of fitting the polarized Raman spectra corresponding to oblique phonon modes of a $Pb_{0.97}Ca_{0.03}TiO_3$ single crystal with model (1). Good agreement of experimental values (circles) with the results of fitting (solid lines) with a sum of additive oscillators is readily seen.

3. EXPERIMENTAL RESULTS AND DISCUSSION

3.1. Dynamic Properties of PbTiO$_3$ and CaTiO$_3$ at Room Temperature

Because studies of the Raman spectra of pure single-crystal CaTiO$_3$ and PbTiO$_3$ have been published before, we will first do an overview of the main results obtained in order to demonstrate the consistency of our spectra with the published data and ensure appropriate interpretation of the specific features observed in the spectra of the solid solutions of these compounds. The polarized Raman spectra of our samples of PbTiO$_3$ and CaTiO$_3$ single crystals at room temperature are displayed in Fig. 1. These spectra adequately reflect the essential structural differences of the two compounds.

The mode assignment for lead titanate was made according to [11, 12]. At room temperature, lead titanate has a primitive tetragonal cell with one formula unit and C_{4v}^1 crystal symmetry. The optical phonon modes of the center of the Brillouin zone transform like the $3A_1 + B_1 + 4E$ symmetry types. Three pairs of A_1 and E phonons originate from threefold degenerate F_{1u} modes of the high-temperature cubic phase. One E mode and one B_1 mode stem from the so-called silent mode of F_{2u} paraphase symmetry, which is active neither in Raman nor in IR spectra.

Long-range electrostatic forces split all $A_1 + E$ modes into transverse optical (TO) and longitudinal optical (LO) components in the ferroelectric phase. The lowest frequency phonons E(1TO) and A_1(1TO) are known as soft modes, because they originate from the F_{1u}(TO) soft mode of the cubic phase [11–14]. The

768
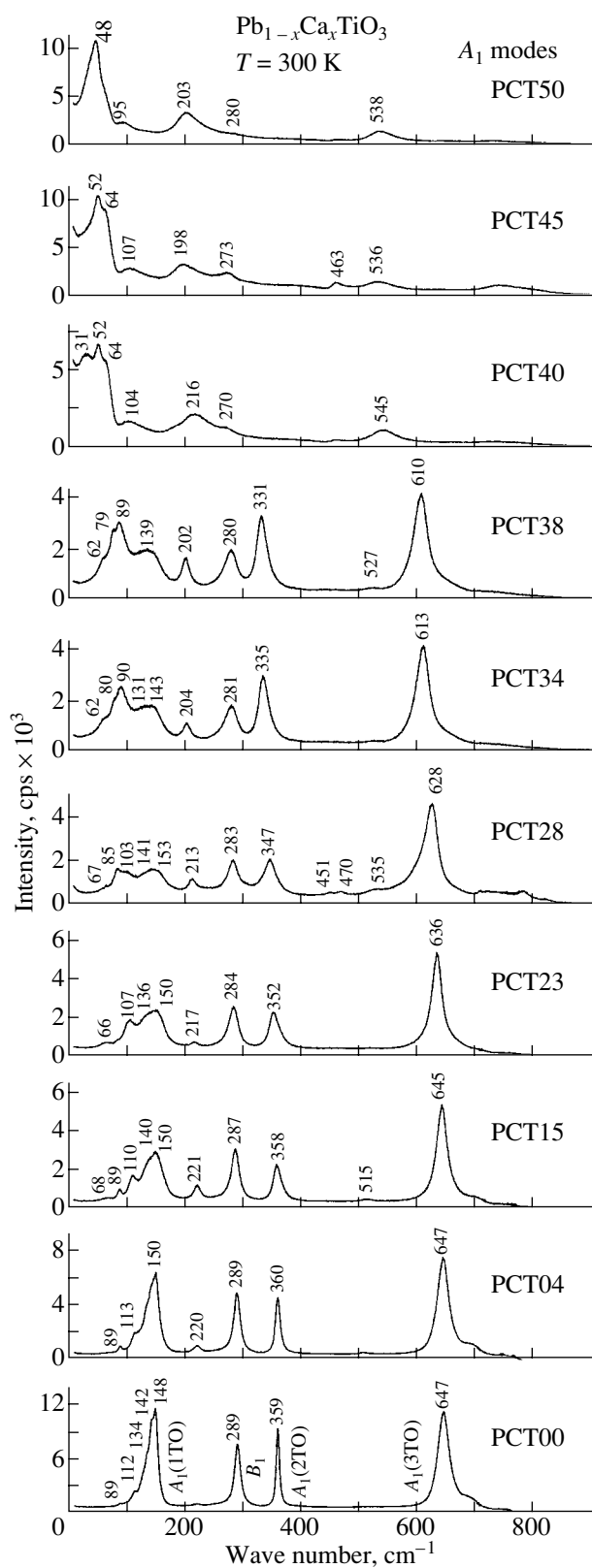
Fig. 4. Evolution of the Raman spectral response corresponding to A_1-type modes in $Pb_{1-x}Ca_xTiO_3$ solid solution crystals with variations in the concentration. The spectral distribution is seen to change strongly when changing over from $Pb_{0.62}Ca_{0.38}TiO_3$ to $Pb_{0.6}Ca_{0.4}TiO_3$, which is an indication of a concentration phase transition in the range $0.38 < x < 0.40$.
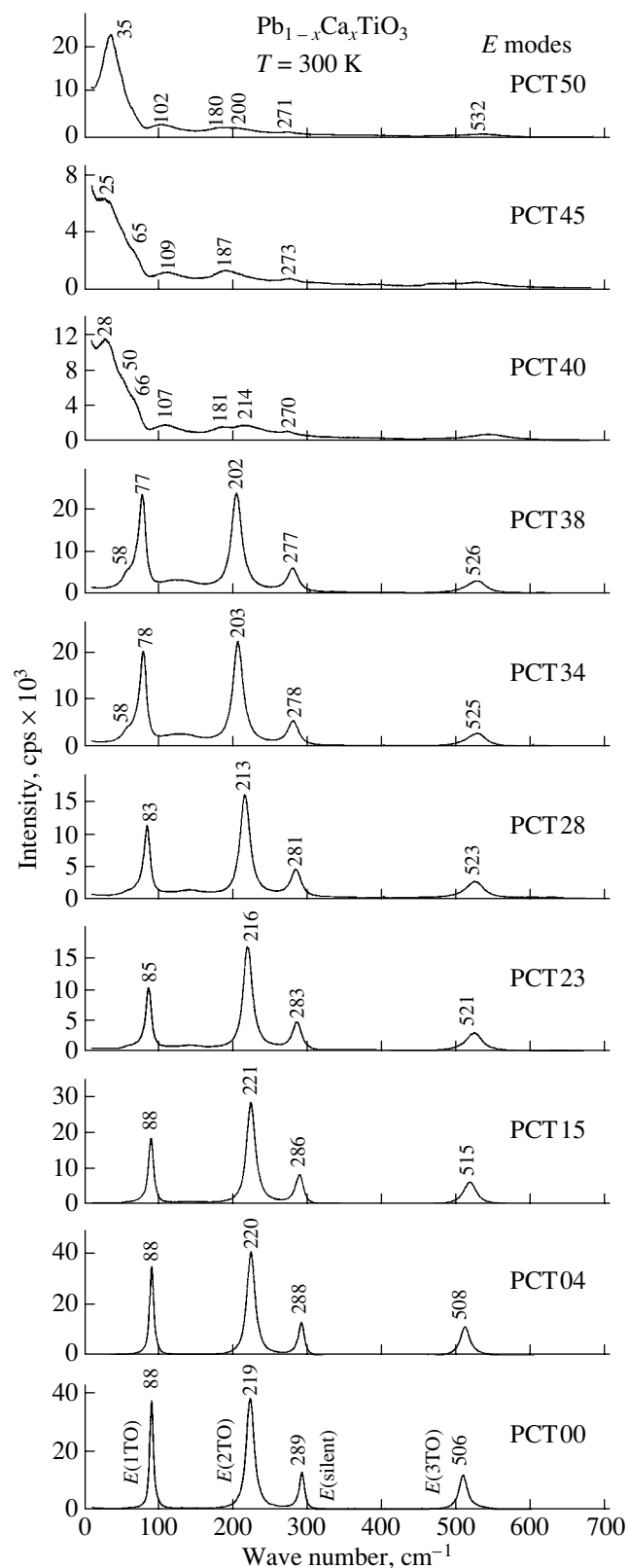
Fig. 5. Evolution of the Raman spectral response corresponding to E-type modes in $Pb_{1-x}Ca_xTiO_3$ solid solution crystals with variations in the concentration. Radical transformation of the spectral distribution upon changing over from $Pb_{0.62}Ca_{0.38}TiO_3$ to $Pb_{0.6}Ca_{0.4}TiO_3$ is clearly visible.
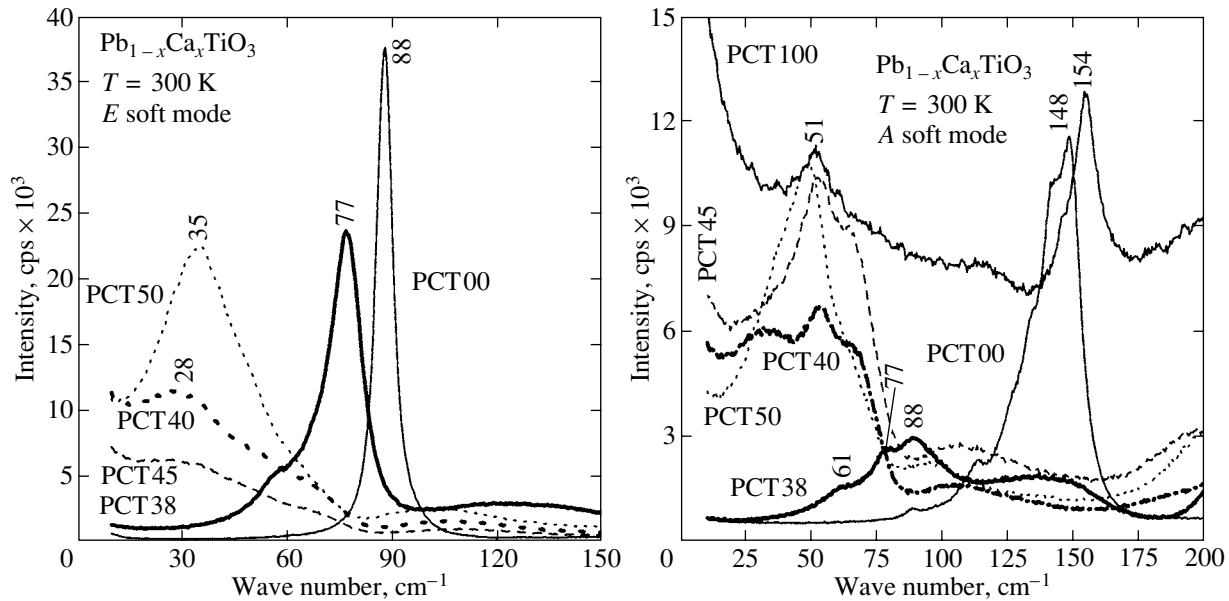
Fig. 6. Evolution of the room-temperature Raman spectral response corresponding to soft modes in PCT solid solution crystals with variations in the concentration near the concentration phase transition in the range $0.38 < x < 0.40$. The spectra of pure lead and calcium titanates are displayed for comparison (thin solid lines). A radical change in the spectral distribution upon changing over from $Pb_{0.62}Ca_{0.38}TiO_3$ to $Pb_{0.6}Ca_{0.4}TiO_3$ is clearly visible (heavy solid lines).

A_1(1TO) component of the soft mode has a complex profile that has been described earlier in [13, 18, 19]. The corresponding profile for our $PbTiO_3$ sample is displayed in Fig. 2. It was unfolded using Eq. (1) into constituents the eigenfrequencies of which are likewise specified in Fig. 2.

The assignment of the phonons of both the LO and TO modes [11, 12] in the ferroelectric phase is valid in the case in which the wave vector is parallel to one of the principal crystallographic axes. For phonons propagating between the principal axes, the A_1 and E modes mix to produce "quasi-modes" in the spectra. These oblique phonons in lead titanate were studied earlier for different directions of propagation [13]. Figure 3 presents such modes observed in a $Pb_{0.97}Ca_{0.03}TiO_3$ crystal. Also shown is a fit of model (1) to the experimental data. A comparison of the spectra of $PbTiO_3$ in Figs. 1–3 with data available in the literature [11–13] suggests that they are identical, within the limits of experimental error.

The phase distortions occurring in the $CaTiO_3$ structure at high temperatures through the rotational mechanism result in Brillouin zone folding and phonon transfer from the points R, M, and X of the cubic Brillouin zone to the center of the orthorhombic Brillouin zone [31]; in this case, the spectrum attributed to the Γ point of the Brillouin zone of orthorhombic $CaTiO_3$ (D_{2h}^{16}) is enriched by new lines as compared to the spectrum of perfect perovskite. The corresponding correlations of symmetry types [31] suggest that all Raman-active phonons in $CaTiO_3$ originate from modes of the Bril-

louin zone edges of the cubic phase. Thus, at room temperature, one may expect a Raman spectrum to consist of 24 lines partitioned among different symmetry types as $7A_g + 5B_{1g} + 7B_{2g} + 5B_{3g}$ and plus 25 polar phonons $9B_{1u} + 7B_{2u} + 9B_{3u}$, which are active only in IR absorption spectra because of the crystal being centrosymmetric (the "mutual exclusion selection rule").

Figure 1b presents the polarized Raman spectra of calcium titanate at room temperature in different scattering geometries. The spectra are slightly depolarized because of the complex domain structure of the sample. One clearly sees a dominant feature in the phonon density of states, against which narrow lines of the first-order spectrum stand out. The Raman response of our $CaTiO_3$ single crystal resembles the corresponding spectrum of single-crystal $CaTiO_3$ reported in [9] while differing somewhat (particularly in the low-frequency range) from the spectra measured for polycrystals [32–34].

The first-principles calculations of the soft mode frequency for calcium titanate were performed in a number of works. It was found that the frequency of the soft polar mode for cubic calcium titanate at $T = 0$ is imaginary and equal to $153i$ [35] and $140i$ cm⁻¹ [36]. This means that, if there were no rotational phase transitions in cubic calcium titanate, this crystal would be a ferroelectric with a fairly high ferroelectric transition temperature. The same calculations made for the orthorhombic phase yield about 90 cm⁻¹ for the soft mode frequency [36]. Pseudopotential calculations [36] permit assignment of the first-order resonance peaks for our $CaTiO_3$ sample. We first note, however, that, because the crystallographic orientation of the domain
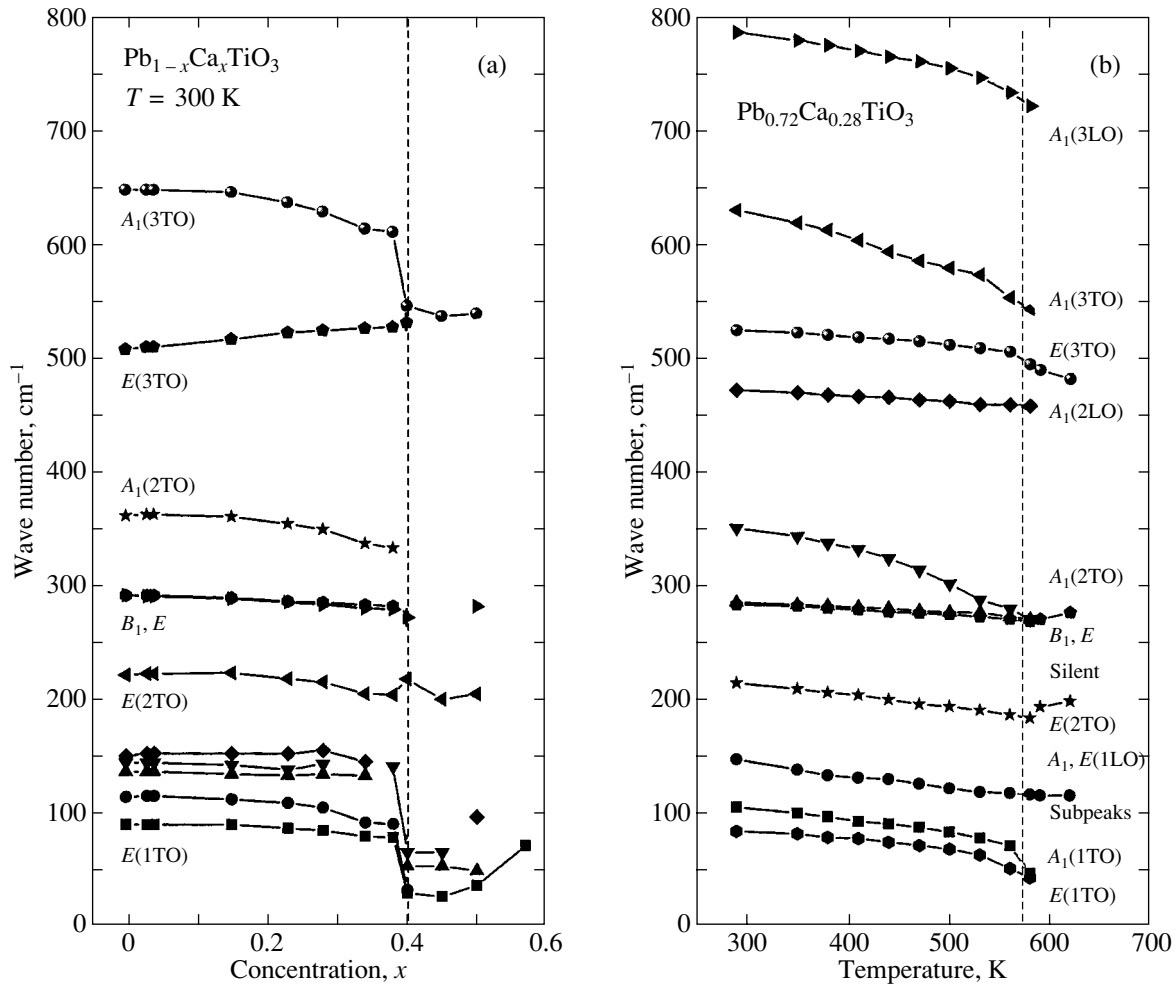
Fig. 7. Comparison of the behaviors of the eigenfrequencies of phonon modes in $Pb_{1-x}Ca_xTiO_3$ solid solution crystals: (a) concentration dependences of the eigenfrequencies of transverse phonons at 300 K (different symbols). The dashed line at $x \approx 0.39$ identifies the phase transition. (b) Temperature dependences of the eigenfrequencies of phonon modes in $Pb_{0.72}Ca_{0.28}TiO_3$ (mode type identified to the right of the corresponding curve). In the cubic phase (the phase transition point is specified by the vertical dashed line), first-order Raman scattering is forbidden by selection rules; therefore, the specified frequencies correspond to maxima in the phonon density of states in the relevant frequency ranges.

from which the micro-Raman response had been obtained was not determined with a high enough precision, the only thing that can be done presently is to unambiguously separate from one another pairs of types (A_g and B_{2g}) and (B_{1g} and B_{3g}). A similar difficulty appeared for isostructural $CdTiO_3$ [37]. In theory, the A_g and B_{2g} modes have frequencies of 100, 139, 225, 268, 314, 446, and 533 and 137, 162, 195, 346, 431, 469, and 774 cm^{-1}, respectively. Analysis of the experiment performed for one crossed (HV) and three parallel (HH, TT, VV) scattering geometries suggests the following correspondence for these types: [155(149), 225(229), 247(252), 284(289), 471(470), 633(613), 662(668)] and [155(140,163), 182(185), 336(343), 457(459), 492(496), 795(797)]. The values in the parentheses are those obtained at 10 K. The spectra corresponding to the B_{1g} and B_{3g} symmetries are characterized by a low intensity and are not discussed here,

because their assignment would require a more careful investigation. It appears obvious, however, that the agreement between the theoretical (calculated by the pseudopotential method) and experimental frequencies is far from being satisfactory, particularly for the totally symmetric modes.

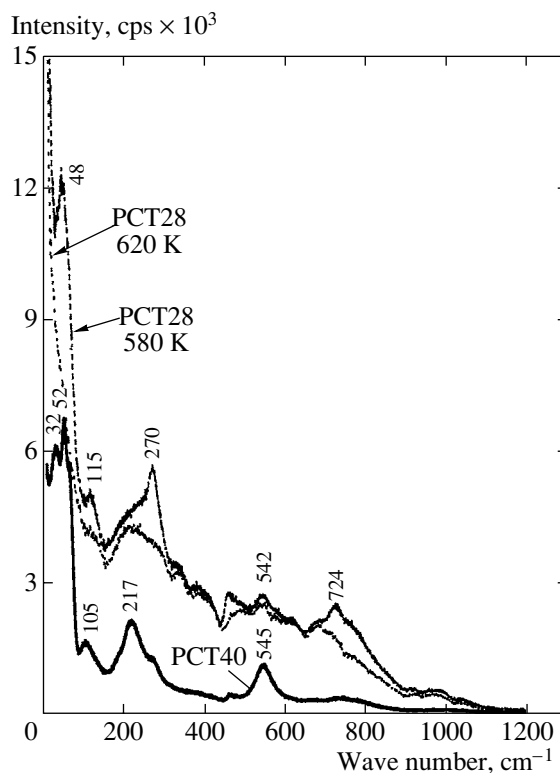### 3.2. Raman Spectra of Mixed $Pb_{1-x}Ca_xTiO_3$ Crystals: Concentration Phase Transition

Figures 4 and 5 demonstrate the spectral evolution of the Raman response corresponding to the A_1 and E modes in $Pb_{1-x}Ca_xTiO_3$ solid solution crystals. Up to $x = 0.38$, the spectral pattern is seen to remain, on the whole, unchanged, but numerical values of the oscillator parameters, namely, the eigenfrequencies ν_i of most modes, decrease, while the damping constants γ_i
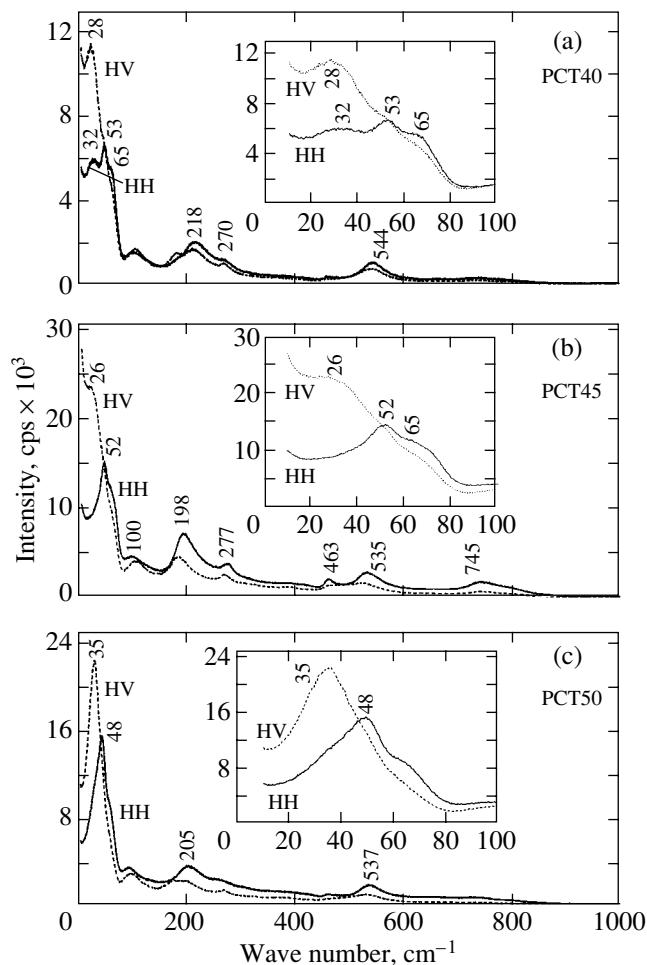
Fig. 8. Polarized Raman spectra of three single crystals of $Pb_{1-x}Ca_xTiO_3$ solid solutions at room temperature in two mutually orthogonal scattering geometries: (a) $Pb_{0.6}Ca_{0.4}TiO_3$, (b) $Pb_{0.55}Ca_{0.45}TiO_3$, and (c) $Pb_{0.5}Ca_{0.5}TiO_3$. Insets show the spectral distribution in the low-frequency range.

Fig. 9. Comparison of the spectral distributions of $Pb_{0.72}Ca_{0.28}TiO_3$ solid solution crystals near the temperature of the phase transition from the tetragonal to cubic state with the Raman spectrum of a $Pb_{0.6}Ca_{0.4}TiO_3$ crystal at room temperature.

increase with increasing x (these graphs are not presented here).

When changing over from $Pb_{0.62}Ca_{0.38}TiO_3$ to $Pb_{0.6}Ca_{0.4}TiO_3$, one observes a sharp change in the character of the spectral distribution both at high (Figs. 4, 5) and, particularly, at low frequencies (Fig. 6). Figure 7 shows the concentration dependences of the eigenfrequencies of transverse phonons at 300 K. Practically all the modes exhibit a slight softening with increasing x, except for the E(3TO) mode, which hardens with increasing x. Near $x \approx 0.4$, one observes frequency jumps, which are particularly pronounced for low-frequency phonons. This transformation obviously reflects the onset of a concentration phase transition (most likely, of first order) in the range $0.38 < x < 0.40$. A comparison of our data with the results of measurements performed with ceramic samples [32] suggests only a certain qualitative resemblance of the spectral

responses at $x < 0.40$ but a radical difference at $x > 0.40$. We will now present supporting evidence for the assumption that the phase state (or states) setting in this case can be identified with neither cubic [20, 32] nor Pnm–D_{2h}^{16} symmetry, as maintained in [28].

Figure 8 plots the Raman phonon spectral responses for solid solutions of three compositions with $x \geq 0.40$. Each case is exemplified by spectra obtained for two mutually orthogonal polarizations of scattered light. The spectra are seen to be well polarized, although the lines are heavily broadened and overlap. To make the spectra more revealing, insets with low-frequency spectra are provided too. A comparison of the spectra in Fig. 8 with those of calcium titanate (Fig. 1) suggests that this spectral distribution is inconsistent with the $Pnma$–D_{2h}^{16} symmetry group, the assignment made for $Pb_{0.5}Ca_{0.5}TiO_3$ in [28]. To provide more convincing evidence for this spectral pattern being inconsistent with cubic symmetry, Fig. 9 compares the spectral distributions obtained for the $Pb_{0.72}Ca_{0.28}TiO_3$ solid solution near the temperature of the phase transition from the tetragonal to cubic state (this first-order transition is observed at $T_c \approx 585$ K, which is evidenced by an abrupt disappearance of the soft mode at 48 cm^{-1}) with the
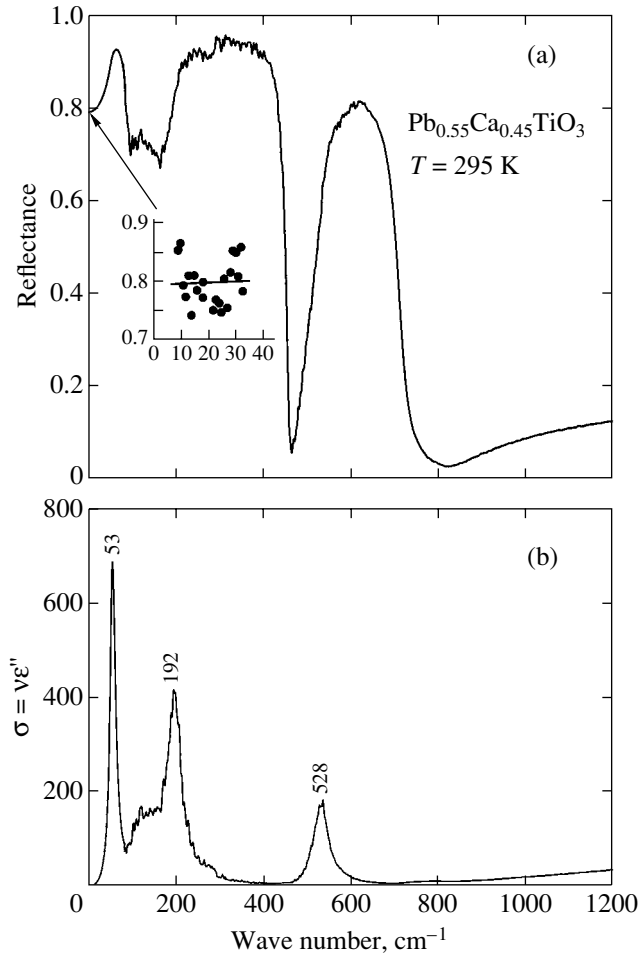
Fig. 10. (a) IR reflectance spectrum $R(\nu)$ of a $Pb_{0.55}Ca_{0.45}TiO_3$ single-crystal plate at 295 K in the frequency range $30 \leq \nu \leq 1200$ cm^{-1} and (b) the dielectric spectrum of the optical conductivity $\sigma = \nu\varepsilon''(\nu)$ derived from the IR reflectance spectrum by the Kramers–Kronig transformation. The inset shows reference values of R obtained from direct measurements in the submillimeter range by BWO spectroscopy.

Raman spectrum of a $Pb_{0.6}Ca_{0.4}TiO_3$ single crystal at room temperature. We clearly see that, above the phase transition temperature, first-order lines (denoted in Fig. 9 by numerical values of the corresponding natural phonon frequencies) are no longer present in the spectra. Since first-order Raman scattering in the cubic phase is forbidden by selection rules, the spectrum at 620 K actually reflects the phonon density of states for the cubic paraphase and the spectra exhibit a strong Rayleigh scattering tail, which evidences, similar to pure $PbTiO_3$ [16, 17], a substantial contribution of the order–disorder-type component to the low-frequency spectral response. As is seen from Fig. 9, the spectrum of the cubic phase differs radically from that of the $Pb_{0.6}Ca_{0.4}TiO_3$ crystal, in which the first-order lines dominate, particularly at low frequencies.

The IR reflectance spectra measured for the $Pb_{0.55}Ca_{0.45}TiO_3$ crystal at 295 K and shown in Fig. 10 can serve as another proof of the phase states for intermediate compositions with $x \geq 0.4$ being neither cubic nor orthorhombic with the $Pnma$–D_{2h}^{16} centrosymmetric group. A comparison of the oscillator parameters (primarily eigenfrequencies) of phonon modes, which were derived from the IR reflectance spectra $R(\nu)$ and calculated according to the Kramers–Kronig relations from the dielectric spectra $\varepsilon'(\nu)$ and $\sigma = \nu\varepsilon''(\nu)$ for a $Pb_{0.55}Ca_{0.45}TiO_3$ single-crystal platelet at 295 K (Fig. 10), with the eigenfrequencies of Raman-active phonons (Fig. 8), suggests that they coincide within the limits of experimental error. This gives grounds to maintain that the phase of the $Pb_{0.55}Ca_{0.45}TiO_3$ composition at room temperature does not have a center of symmetry and, hence, can be polar (because of lifting of the mutual exclusion selection rule).

Finally, we note the differences between the concentration and temperature dependences of the oscillator parameters of the $Pb_{0.72}Ca_{0.28}TiO_3$ composition used as an example (Fig. 7). First, in the temperature dependence, unlike the concentration dependence, the frequency of the A_1(2TO) mode merges with the frequency of the silent mode near the temperature-induced phase transition at $T_c \approx 585$ K (Fig. 7b). Second, as one approaches the concentration phase transition at $x \approx 0.40$, the frequency of the E(3TO) mode increases, whereas upon the temperature-induced transition to the cubic phase state, it decreases (compare Figs. 7a and 7b).

The above observations provide compelling evidence that, at room temperature, the phase states of samples with $x \geq 0.4$ have not a cubic but a lower symmetry and are different from the tetragonal structure of lead titanate and the centrosymmetric structure of calcium titanate, a conclusion definitely at odds with the opinions expressed, in particular, in [29, 32].

Optical studies [30] suggest the existence of more than one phase with a complex phase diagram at medium concentrations. It is argued [30] that the phase with $x \geq 0.4$ is ferroelectric at room temperature (which is in accord with its dielectric hysteresis [20, 21] and with our dynamics data). Our next paper will study in considerable detail the spectra of $Pb_{0.55}Ca_{0.45}TiO_3$ and analyze the possible composition of these phase states.

4. CONCLUSIONS

The dynamic behavior of PCT solid solutions in the frequency range of optical phonons is studied using single-crystal samples for the first time. The spectrum of the crystals with $0 < x < 0.4$ is qualitatively similar to that of the tetragonal $PbTiO_3$. The spectrum of samples with $x \geq 0.4$ differs radically. It is dominated at low frequencies by a strong, heavily structured resonance line with a frequency coinciding, within the limits of experimental error, with its IR analogue, which suggests a possible polar character of the new phase state. This suggestion

is in conflict with earlier reports of the PCT solid solutions having cubic symmetry [20, 32] in the medium concentration range. We have not observed any evidence for the relaxor phase state of our samples in phonon spectral responses of the crystal compositions studied here.

ACKNOWLEDGMENTS

REFERENCES

1. T. Vogt and W. W. Schmahl, Europhys. Lett. **24**, 281 (1993).
2. T. Matsui, H. Shigematsu, Y. Arita, Y. Hanajiti, N. Nakamitsu, and T. Nagasaki, J. Nucl. Mater. **247**, 72 (1997).
3. M. Ahtee, A. Glaser, and A. Hewat, Acta Crystallogr., Sect. B: Struct. Crystallogr. Cryst. Chem. **34**, 752 (1978).
4. B. J. Kennedy, C. J. Howard, and B. C. Chakoumakos, J. Phys.: Condens. Matter **11**, 1479 (1999).
5. H. F. Kay and P. C. Bailey, Acta Crystallogr. **10**, 219 (1957).
6. W. Cochran and A. Zia, Phys. Status Solidi **25**, 273 (1968).
7. V. V. Lemanov, A. V. Sotnikov, E. P. Smirnova, M. Weihnacht, and R. Kunze, Solid State Commun. **110**, 611 (1999).
8. A. S. Knyazev, Yu. M. Poplavko, V. P. Zakharov, and V. V. Alekseev, Fiz. Tverd. Tela (Leningrad) **15**, 3006 (1973) [Sov. Phys. Solid State **15**, 2003 (1973)].
9. V. Zelezny, E. Cockayne, J. Petzelt, M. F. Limonov, D. E. Usvyat, V. V. Lemanov, and A. A. Volkov, Phys. Rev. B: Condens. Matter **66**, 224303 (2002).
10. G. Shirane, S. Hoshino, and K. Suzuki, Phys. Rev. **80**, 1105 (1950).
11. G. Burns, and B. A. Scott, Phys. Rev. Lett. **25**, 167 (1970).
12. G. Burns, and B. A. Scott, Phys. Rev. B: Solid State **7**, 3088 (1973).
13. C. M. Foster, Z. Li, M. Grimsditch, S.-K. Chan, and D. J. Lam, Phys. Rev. B: Condens. Matter **48**, 10160 (1993).
14. G. Shirane, J. D. Axe, J. Harada, and J. P. Remeika, Phys. Rev. B: Solid State **2**, 155 (1970).
15. J. A. Sanjurjo, E. Lopez-Cruz, and G. Burns, Phys. Rev. B: Condens. Matter **28**, 7260 (1983).
16. N. Sicron, B. Ravel, Y. Yacoby, E. A. Stern, F. Dogan, and J. J. Rehr, Phys. Rev. B: Condens. Matter **50**, 13168 (1994).
17. M. D. Fontana, H. Idrissi, G. E. Kugel, and K. Wojcik, J. Phys.: Condens. Matter **3**, 8695 (1991).
18. S. M. Cho and H. M. Jang, Appl. Phys. Lett. **76**, 3014 (2000).
19. S. M. Cho, H. M. Jang. and T. Y. Kim, Phys. Rev. B: Condens. Matter **64**, 014103 (2001).
20. E. Sawaguchi and M. J. Charters, J. Am. Ceram. Soc. **42**, 157 (1959).
21. T. Yamamoto, M. Saho, K. Okazaki, and E. Goo, Jpn. J. Appl. Phys. **26–2** (Suppl.), 57 (1987).
22. B. Jiménez and R. Jiménez, Phys. Rev. B: Condens. Matter **66**, 014104 (2002).
23. A. Seifert, P. Muralt, and N. Setter, Appl. Phys. Lett. **72**, 2409 (1998).
24. S. G. Moorthy, S. Balakumar, F. J. Kumar, C. Subramanian, and P. Ramasamy, Mater. Chem. Phys. **57**, 281 (1999).
25. X. G. Tang, A. L. Ding, H. Q. Li, and D. Mo, J. Non-Cryst. Solids **297**, 67 (2002).
26. R. Poyato, M. L. Calzada, and L. Pardo, J. Appl. Phys. **93**, 4081 (2003).
27. V. V. Lemanov, A. V. Sotnikov, E. P. Smirnova, and M. Weihnacht. Appl. Phys. Lett. **81**, 886 (2002).
28. R. Ranjan, N. Singh, D. Pandey, V. Siruguri, P. S. R. Krishna, S. K. Paranjpe, and A. Banerjee, Appl. Phys. Lett. **70**, 3221 (1997).
29. R. Ganesh and E. Goo, J. Am. Ceram. Soc. **80**, 653 (1997).
30. V. V. Eremkin, V. G. Smotrakov, L. E. Balyunis, S. I. Shevtsova, and A. T. Kozakov, Kristallografiya **39** (1), 155 (1994) [Crystallogr. Rep. **39** (1), 137 (1994)].
31. A. A. Volkov, G. A. Komandin, B. P. Gorshunov, V. V. Lemanov, and V. I. Torgashev, Fiz. Tverd. Tela (St. Petersburg) **46** (5), 899 (2004) [Phys. Solid State **46** (5), 927 (2004)].
32. S.-Y. Kuo, C.-T. Li, and W.-F. Hsieh, Phys. Rev. B: Condens. Matter **69**, 184104 (2004).
33. U. Balachandran and N. G. Eror, Solid State Commun. **44**, 815 (1982).
34. P. Gillet, F. Guyot, G. D. Price, B. Tournerie, and A. Le Cleach, Phys. Chem. Miner. **20**, 159 (1993).
35. W. Zhong, R. D. King-Smith, and D. Vanderbilt, Phys. Rev. Lett. **72**, 3618 (1994).
36. E. Cockayne and B. P. Burton, Phys. Rev. B: Condens. Matter **62**, 3735 (2000).
37. V. I. Torgashev, Yu. I. Yuzyuk, V. B. Shirokov, V. V. Lemanov, and I. E. Spektor, Fiz. Tverd. Tela (St. Petersburg) **47** (2), 324 (2005) [Phys. Solid State **47** (2), 337 (2005)].

Translated by G. Skrebtsov